

Graph method for critical pipe analysis of branched and looped drainage networks

Aun Dastgir , Sina Hesarkazzazi, Martin Oberascher, Mohsen Hajibabaei and Robert Sitzenfrei *

Unit of Environmental Engineering, Department of Infrastructure Engineering, Faculty of Engineering Sciences, University of Innsbruck, Technikerstrasse 13, Innsbruck 6020, Austria

*Corresponding author. E-mail: robert.sitzenfrei@uibk.ac.at

 AD, 0000-0001-7280-4807; RS, 0000-0003-1093-6040

ABSTRACT

Enhancing resilience of drainage networks is a crucial practice to protect both humans and nature. One way to enhance resilience is to identify critical parts of drainage networks for targeted management and maintenance strategies. While hydrodynamic modelling approaches for identification are computationally intensive, in this study, a novel method based on complex network analysis is used to determine the most critical pipes in a benchmark and a real network of an Alpine municipality. For evaluation, the results of the proposed graph method are compared with hydrodynamic simulations in terms of accuracy and computational time. Results show that the proposed method is very accurate ($R^2 = 0.98$) for branched benchmark network while the accuracy reduces slightly for the more complex real network ($R^2 = 0.96$). Furthermore, the accuracy of the proposed method decreases with increasing loop degree and when the system is pressured with higher return period rainfall. Although the outcomes of the proposed method show slight differences to hydrodynamic modelling, it is still very useful because the computational time and data required are much less than a hydrodynamic model.

Key words: complex network analysis, edge betweenness centrality, graph theory, hydrodynamic modelling, pipe criticality, shortest path

HIGHLIGHTS

- A graph-based framework tailored to hydraulic characteristics of drainage networks is developed.
- The presented methodology is very accurate for small tree-like networks but accuracy decreases with increasing complexity, loop degree and return period of rain.
- The proposed graph-based method is computationally efficient and requires less data.
- Hybrid method, a combination of two methods, combines both advantages.

INTRODUCTION

Urban stormwater networks (USNs) are considered to be an important infrastructure for life in urban areas. These systems convey stormwater away from urban areas and contribute to the general well-being of the population (Fu *et al.* 2011). Following, a structural (e.g., blockage induced) and functional (e.g., precipitation induced) failure are two commonly adopted failure modes in USNs, which can greatly affect the performance of such systems (Butler *et al.* 2017). USNs are interconnected infrastructure and therefore considered complex networks, hindering the straightforward design, management, and operation of these systems. The challenges increase when considering also climate change, population increase, urbanization and aging elements which can lead to financial and mortal threats (Dong *et al.* 2017). To achieve a high serviceability desired for USNs, they have to be maintained and rehabilitated regularly (Le Gauffre *et al.* 2007). Considering these challenges, it is important to make USNs more resilient. Resilience of USNs can be defined as its ability to minimize damage and rapidly recover from extreme loading conditions by lessening failure consequences (Mugume & Butler 2017). Therefore resilience-boosting intervention strategies should be applied to USNs to deal with both normal and extreme loading scenarios.

An efficient yet effective way of enhancing resilience of any infrastructure is to identify its most important elements to focus on these critical elements in management and maintenance strategies, hence increasing the overall system's resilience. The overall performance of the stormwater network depends on the performance of its individual elements. Characteristics of a particular element and its position in the USN contribute to the importance of such element (Meijer *et al.* 2018). Maintaining

This is an Open Access article distributed under the terms of the Creative Commons Attribution Licence (CC BY 4.0), which permits copying, adaptation and redistribution, provided the original work is properly cited (<http://creativecommons.org/licenses/by/4.0/>).

all the elements to the same high service level is expensive in terms of cost and resources required. If the degree of criticality of different elements of a USN is known, the elements with higher degree of criticality can be given priority for maintenance and rehabilitation to increase the system's resilience while decreasing the associated costs. The degree of criticality can therefore be used as a basis for risk-based asset management (Meijer *et al.* 2018). Risk assessment includes two parts, consequence of failure and probability of failure. The aim of this study is to focus on the aftermaths of failure and hence, only the consequence of failure part of the risk assessment is considered.

There exist only a handful of methodologies to identify critical elements in a stormwater network in literature. Arthur & Crow (2007) worked on a methodology to find critical elements based on serviceability loss after the failure. The pipes are ranked on the basis of combination of consequence scoring (depending on consequence of failure) and likelihood scoring (based on likelihood of failure). Möderl *et al.* (2009) presented the development and application of the software tool VulNetUD, which is a tool for GIS based identification of vulnerable sites of drainage networks. The tool uses the Storm Water Management Model (SWMM). Another methodology for this purpose frequently used in literature is called the Achilles approach, (Möderl *et al.* 2009; Möderl & Rauch 2011; Sitzenfrei *et al.* 2011; Mair *et al.* 2012), where the systematic Hydrodynamic Modelling Method (HMM) is used. Within this approach, the capacity of each conduit is reduced to almost zero one by one to mimic pipe blockage and then the hydraulic consequences such as overall system flooding are determined and pipes are ranked on the basis of flooding produced. Mugume *et al.* (2015) used a similar approach by modelling pipe failure and adding storage tanks in (a) centralized and (b) decentralized manner to gauge the impact on overall system flooding. Zhang *et al.* (2017) used an approach based on HMM for vulnerability analysis of USNs. A performance indicator based on flooding volume and runoff volume is used in this study to rank the pipes. For large networks and looped systems, these methodologies require very high computational time and effort.

To solve the problem of high computational efforts for assessing water networks, researchers have started working with graph theory and complex network analysis to model urban water infrastructure. Graph theory is a branch of mathematics that employs graphs to model complex real-life problems more efficiently (Turan *et al.* 2019). Up to now, graph theory has been widely used to solve different design and modelling problems of urban water infrastructure, such as identification of critical pipes (Pagano *et al.* 2019; Hajibabaei *et al.* 2022) and optimal design of pipes for water distribution networks (Sitzenfrei *et al.* 2020). Exemplary applications of graph theory for urban drainage networks (UDNs) are layout and design (Turan *et al.* 2019; Hesarkazzazi *et al.* 2022a, 2022b), functional analysis (Reyes-Silva *et al.* 2020), assessing redundancy (Hesarkazzazi *et al.* 2022a, 2022b) and assessing the efficiency of different topological positions of combined sewer overflow structures in a UDN (Sitzenfrei *et al.* 2013). Meijer *et al.* (2018) has described a method for finding critical elements of UDN based on graph theory, which focuses on comparing the costs of the graph by removing the pipes one by one. Head loss is used as weight and shortest path length as graph measure to find the critical pipes in this research. The critical pipes are recognized based on the cost associated with the graph after removing a particular pipe. The method is repeated for all the pipes and the pipe that results in the highest graph cost when removed is considered the most critical pipe and so on. However, there is a need to extend the aforementioned research for finding critical pipes to a non-iterative graph methodology to save the computational time and effort in the case of large, complex USNs and when a lot of simulations have to be made. The scheme mentioned in this study enforces an easy-to-implement method which can be easily extended to multiple pipe failures or cascading failures.

Recognizing the research gap, this paper proposes a new method based on graph theory and complex network analysis to identify the critical pipes of a USN. In contrast to the conventional hydrodynamic modelling method, the proposed method does not depend on iterative simulations which is a time-consuming procedure. Instead, it employs the concept of network analysis to mimic functional and hydraulic properties of USNs. Critical pipes are identified with a graph-based measure called Runoff Edge Betweenness Centrality (EBC_e^R) which can be interpreted as flooding volume by multiplying it with rainfall volume for a particular pipe when that pipe is blocked. This research focuses on both tree and looped networks and also discusses the impact of loop degree on the accuracy of the method. Finally, the results from the graph-based method (GBM) are compared with hydrodynamic modelling method (HMM) in terms of accuracy, computational time, and effort required.

MATERIALS AND METHODS

Graph representation of USNs

A graph G is a set of nodes/vertices (V) and edges (E) and can be represented as $G = (V, E)$, where $V(G)$ is the set of vertices or nodes and $E(G)$ is the set of edges. An edge is represented using an ordered pair of vertices (i, j) where, ' i ' is the source node of

the edge and 'j' is the target node of the edge. A graph is undirected when the graph has no particular direction or it is directed if the edge (i,j) is directed from node i to node j. A graph can be branched if there exists only one unique path between each pair of nodes (no loops) or looped if there exists more than one path between a particular pair of nodes. Additionally, a graph can be weighted, i.e., nodes or edges can have weights. In USNs, manholes, storage tanks, etc. are nodes/vertices of the graph and pipes, pumps and weirs etc. are the edges of the graph. In this study, we will use undirected graphs with weighted edges. Length is used as weight in this study and because length stays the same in both directions for a particular link, using an undirected graph is more convenient for implementing the method as compared to directed graphs, without impacting the results.

The graph measures in this study are modified to the functioning and hydraulic properties of USNs. Shortest path length ($\sigma_{i,j}$) is the first graph measure that is used in this study. It can be defined as the path between two particular nodes (i and j) which has a minimum sum of edge weights or costs associated with the graph (Dijkstra 1959). For calculating the shortest path lengths, the length of a pipe is used as an edge weight in this study. This is because the requirement is to find the shortest path in terms of shortest distance to the outlet from a particular inlet node and to give preference to large pipes with high capacities.

Another graph measure that is used in the study is called Edge Betweenness Centrality (EBC). EBC of a particular edge (pipe) e can be defined as the number of shortest paths between every pair of nodes in a graph that pass through the edge e . To customize this graph measure suitable for USNs, two modification are added to EBC. Therefore, instead of adding 1 for every edge that is part of shortest path, contributing runoff area R_i of each inlet node is added to calculate the EBC values. R_i is calculated by multiplying the area of all the sub catchments connected to a particular node 'i' with their respective percentage imperviousness. Secondly, not all node pairs are considered, only paths between inlet and outlet nodes are considered. This measure is called Runoff Edge Betweenness Centrality (EBC_e^R) (Hesarkazzazi *et al.* 2021) and for edge e is given by:

$$EBC_e^R = \sum_{i,j} \sigma_{i,j}(e) * R_i \quad (1)$$

Another measure proposed in this study is the Capacity Edge Betweenness Centrality (EBC_e^C). EBC_e^C is calculated based on Manning-Strickler formula (Gioia & Bombardelli 2001) and continuity equation using diameter and slope of a pipe and corresponds to the capacity of the pipe e . If an edge is a pump, the design flow is the EBC_e^C value. For pipes, Manning Strickler formula is used to calculate velocities and is given by:

$$V = k * R_h^{2/3} * \sqrt{S} \quad (2)$$

where V = velocity in pipe, k = Strickler coefficient, R_h = hydraulic radius of the pipe and S = slope of the pipe. Using the Manning Strickler equation implies the assumption that the flow is uniform, gravity driven and the equation is derived for open channels. The velocity in the pipe is estimated using this formula and then the continuity equation is used to estimate discharge capacity of each pipe called EBC_e^C . EBC_e^C can also be interpreted as design flows of the pipes, organized in a graph structure and having the same units as EBC_e^R .

$$EBC_e^C = A * V \quad (3)$$

where EBC_e^C = capacity edge betweenness centrality of the pipe, A = area of the pipe and V = velocity of the pipe.

Graph based method (GBM) for critical pipe analysis

Branched network

Flooding volume produced in the system when a particular pipe is blocked can be replicated using GBM. This is achieved by using the concepts of shortest path length and EBC_e^R as described in the section above. The functionality of the approach in the case of a fully branched network is illustrated using a simple network consisting of six nodes and five edges as shown in Figure 1(a).

The first step is to identify the shortest paths from all inlet nodes (1,2,3,4,5) to the outlet node (6) shown in red in the example network. For every node, the pipes that are part of the shortest path get a value of 1 and all other pipes get a

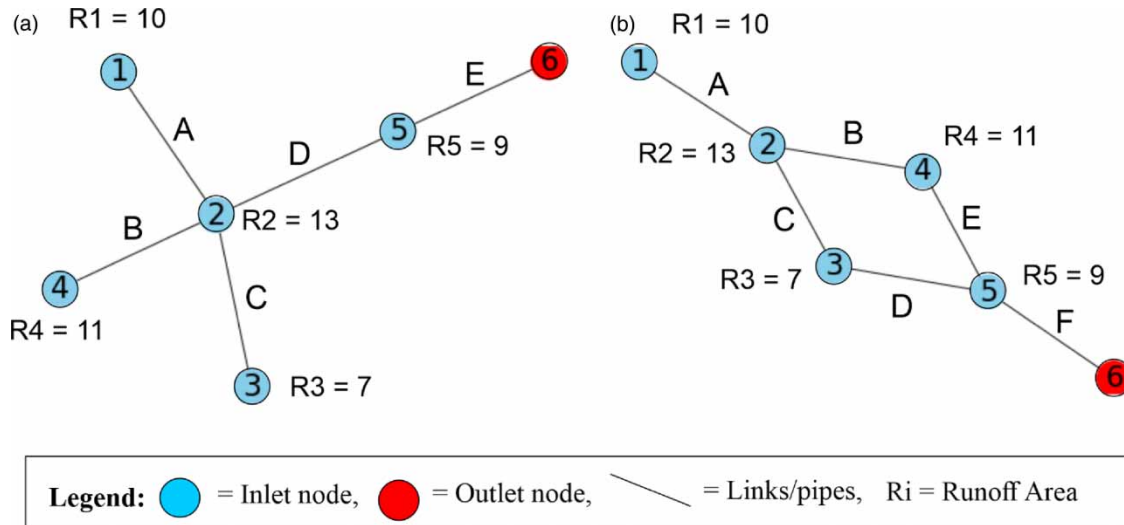


Figure 1 | Exemplary networks, (a) branched, (b) looped.

value of 0 forming a matrix of zeros and ones. EBC of a particular pipe is then calculated by summarizing the row's values associated with that pipe as shown in Table 1.

In the next step, EBC_e^R is calculated to make it more suitable to the use case of USNs (Table 2). Runoff area of each node R is calculated using the area of sub-catchments connected to a particular node and their imperviousness, which is multiplied by all matrix elements in the corresponding shortest path. When a particular row is summed up, EBC_e^R of that pipe is calculated.

For a fully branched network, the EBC_e^R multiplied by rainfall volume corresponds to the flooding volume when that particular pipe is simulated as blocked. This flooding volume is then compared with the flood volume obtained from the HMM method.

Table 1 | Edge betweenness centrality vector for example network in Figure 1(a)

Pipes \ Nodes	1	2	3	4	5	EBC
A	1	0	0	0	0	1
B	0	0	0	1	0	1
C	0	0	1	0	0	1
D	1	1	1	1	0	4
E	1	1	1	1	1	5

Table 2 | Runoff edge betweenness centrality vector for example network in Figure 1(a)

Pipes \ Nodes	1	2	3	4	5	EBC ^R
A	10	0	0	0	0	10
B	0	0	0	11	0	11
C	0	0	7	0	0	7
D	10	13	7	11	0	41
E	10	13	7	11	9	50

Table 3 | Flood volume calculation for example network in Figure 1(b)

Pipes	Nodes					EBC_e^R	EBC_e^C	Flood Volume
	1	2	3	4	5			
A	10	0	0	0	0	10	–	10
B	0	0	0	0	0	0	8	0
C	10	13	0	0	0	23	9	15
D	10	13	7	0	0	30	11	22
E	0	0	0	11	0	11	12	2
F	10	13	7	11	9	50	–	50

Looped network

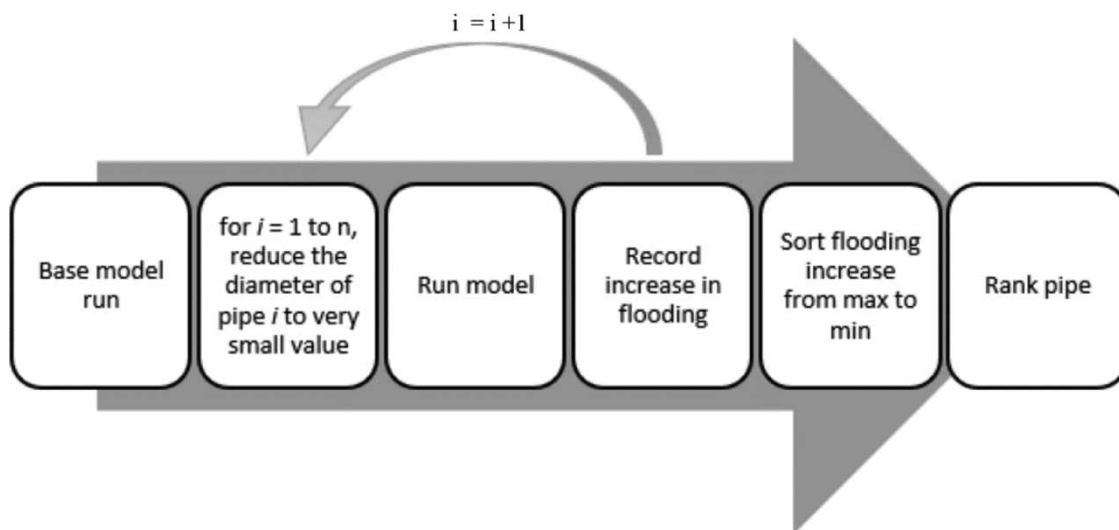
In the case of a looped network, the aforementioned methodology has to be adapted to include the impact of loops on flooding as well. This is done by employing the concept of Capacity Edge Betweenness Centrality (EBC_e^C), given in Equation (3).

In the toy example of a looped network shown in Figure 1(b), nodes 2,3,4 and 5 are part of the loops as they have alternative paths which means even if one of the pipes B, C, D or E are blocked, there is an alternative path for flow to the outlet 6 (shown in red). Capacity and slope of the pipe in an alternate path influence the amount of flow that can be redirected. Table 3 shows the methodology for flood calculation of a looped network. If pipe C is blocked in the above example, whole EBC_e^R value of pipe C (23) does not correspond to flood volume, rather a portion or all of it can be redirected to pipe B. The amount that can be redirected depends on EBC_e^C of the pipe B (8). Flood volume produced when pipe C is blocked can be calculated by subtracting the EBC_e^C value of pipe B from the EBC_e^R value of pipe C, which will be 15 in the case of the example. Similarly, the procedure can be repeated for all the pipes having alternate paths/loops. The pipes are ranked on the basis of flooding volume in the system in case of blockage. The pipe with the highest flood volume is ranked most critical.

Hydrodynamic Modelling Method (HMM) for critical pipe analysis

The results of the GBM are compared with the results of the hydrodynamic modelling method. Therefore, we applied the method developed by Möderl *et al.* (2009) and Mair *et al.* (2012) using the Stormwater Management Model (SWMM) (Rossman 2010). The work flow to determine the critical pipes is shown in Figure 2.

First, a simulation is performed with the initial state (e.g., all pipes have full capacity) called base run. The base run is performed to see if there is any flooding in a fully functional system. Flooding due to the lack of capacity can negatively impact

**Figure 2** | Process to determine critical pipes using hydrodynamic modelling method.

the GBM results. Hence, it is important that for the used rainfall, there is no flooding as capacity problems of the initial system are not in the focus of this study (but will be a part of future studies). Then, the diameter of a single pipe is reduced to a very small value of 1 mm (Mugume *et al.* 2015) to simulate a blockage or failure, while maintaining hydraulic connectivity required for the solution of flow equations. This procedure is then repeated for all the pipes. Subsequently, the number of simulations is equal to the number of pipes plus one. The increase in flood volume is compared to the base run and determined for every pipe blockage. The blocked pipe that causes the highest flooding volume in the system is considered as the most critical pipe. The performance indicator used for this purpose therefore depends on the increase in flooding volume and can be given by:

$$PI = \sum_{I=1}^n V_F \quad (4)$$

in which PI is the performance indicator, n is the number of nodes, and V_F is the flood volume of each node. A higher value of performance indicator indicates a higher flood volume of the blocked pipes and is therefore an indicator for the pipe criticality.

Comparison of criticality between GBM and HMM

The Pearson correlation coefficient (Pearson 1895) and coefficient of determination (R^2) is used to determine the correlation between the results from GBM and HMM in this study. R^2 is calculated by performing linear regression on the data. For our data, which can be categorized as linear rather than monotonic and does not have any significant outliers, Pearson coefficient is most suitable correlation coefficient. Pearson coefficient (r) is a parametric measure that measures the strength and direction of linear relationships in a set of data. The value of ' r ' changes from -1 to 1 , where -1 shows the perfect negative correlation, 1 shows the perfect positive correlation while 0 shows no correlation between the dataset. Pearson correlation coefficient ' r ' can be given by the formula:

$$r = \frac{\sum (xi - \bar{x})(yi - \bar{y})}{\sqrt{\sum (xi - \bar{x})^2 \sum (yi - \bar{y})^2}} \quad (5)$$

where; r = Pearson correlation coefficient; xi = values of the x -variable in the dataset; \bar{x} = mean of the values of the x variable; yi = values of the y -variable in the dataset; \bar{y} = mean of the values of the y variable.

Along with that, to measure the differences between flooding volume values from GBM when compared with HMM, normalized root mean square error (NRMSE) is used in this study. We need this measure because R^2 and r only show how well the data fits and not the difference between actual flooding volume values. GBM results are considered as modeled values and corresponding HMM results as actual values for this purpose. NRMSE value of zero show the perfect result and larger values of NRMSE shows more differences between the two methods. NRMSE can be given by the formula:

$$NRMSE = \frac{\sqrt{\frac{\sum_{n=1}^N (y_n - x_n)^2}{N}}}{y_{max} - y_{min}} \quad (6)$$

where; $NRMSE$ = normalized root mean square error; N = total number of data points (pipes); y_n = Flooding volume from GBM for pipe n ; x_n = Flooding volume from HMM for pipe n ; y_{max} = maximum flooding volume from GBM; y_{min} = minimum flooding volume from GBM.

Case studies

Two different case studies are used to identify the potential of the proposed method. First, a small benchmark network is used consisting of 59 pipes and second, a real network of an Alpine municipality in Austria is used consisting of 373 pipes.

Benchmark network

The benchmark network used in this study is hydraulically designed by [Hesarkazzazi et al. \(2021\)](#) for a block rain event with a return period of two years and a duration of 15 minutes, yielding a total rain volume of 17.1 mm. The network was designed to not produce any flooding for two-year return period rain. The benchmark network is a fully branched network that drains an area of 175 hectares. The network consists of 59 circular pipes connected by 60 nodes including one outlet as shown in [Figure 3](#). The diameters range from 375 mm to 3000 mm.

To extend the study to looped networks, redundant flow paths (forming loops) are created in the benchmark network. Two networks having three (5% loop degree) and six loops (10% loop degree) respectively are created to study the impact of loop degree on the proposed methodology. These loops are not designed, rather slope and length of these pipes are calculated by the SWMM model based on their positioning in the network while the diameters are estimated based on the adjacent pipes. The location of these loops was manually selected based on engineering judgement of only inserting a short connection and preserving a planar graph (no crossings).

Real network

For a real case study, the existing USN of an Alpine municipality is used located in the state of Tyrol in Austria, as shown in [Figure 4](#). It is a fully branched network that comprises 373 links connected by 374 nodes. The diameters range from 250 mm

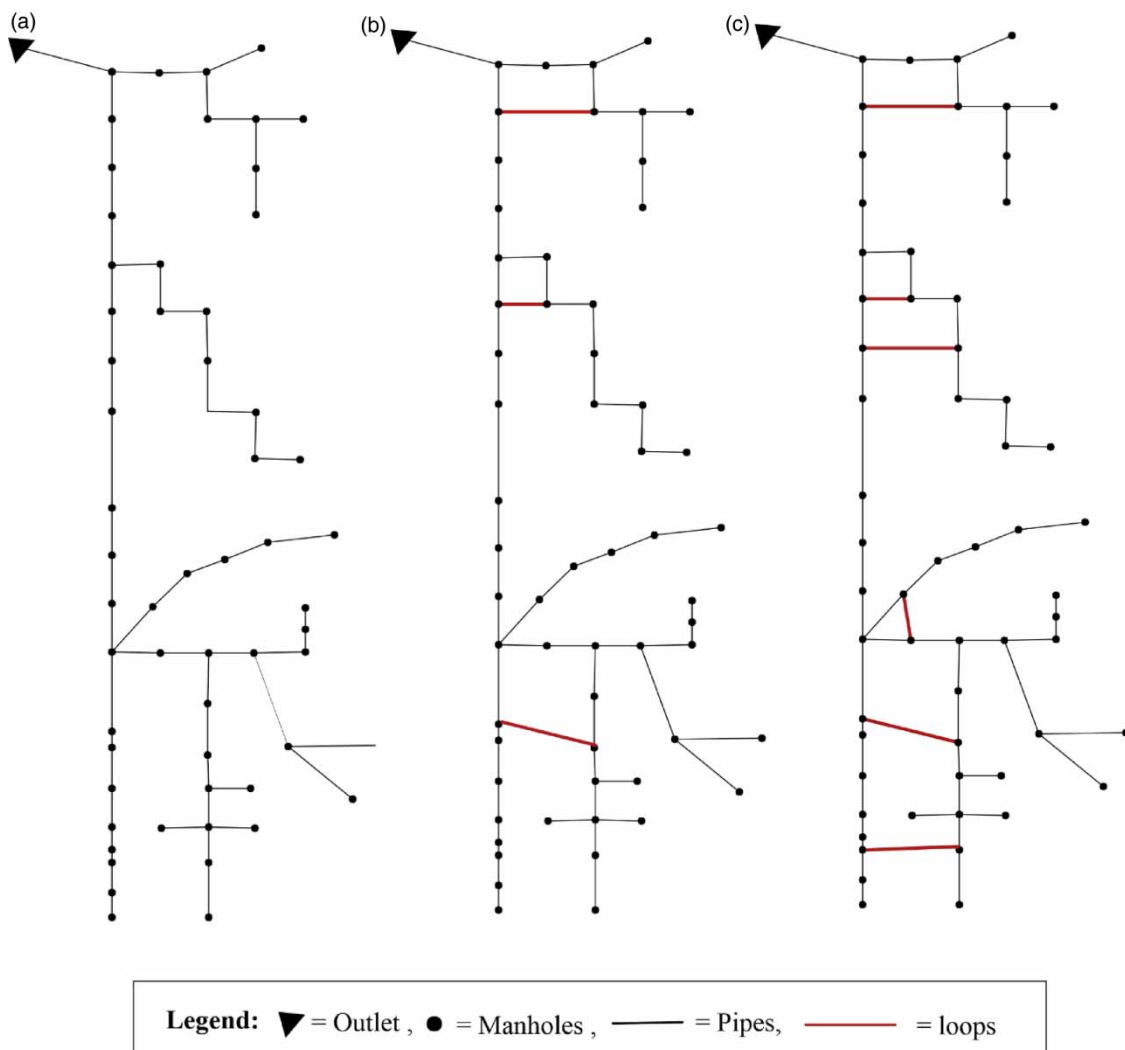


Figure 3 | Benchmark network: (a) original fully branched, (b) three loops, (c) six loops.

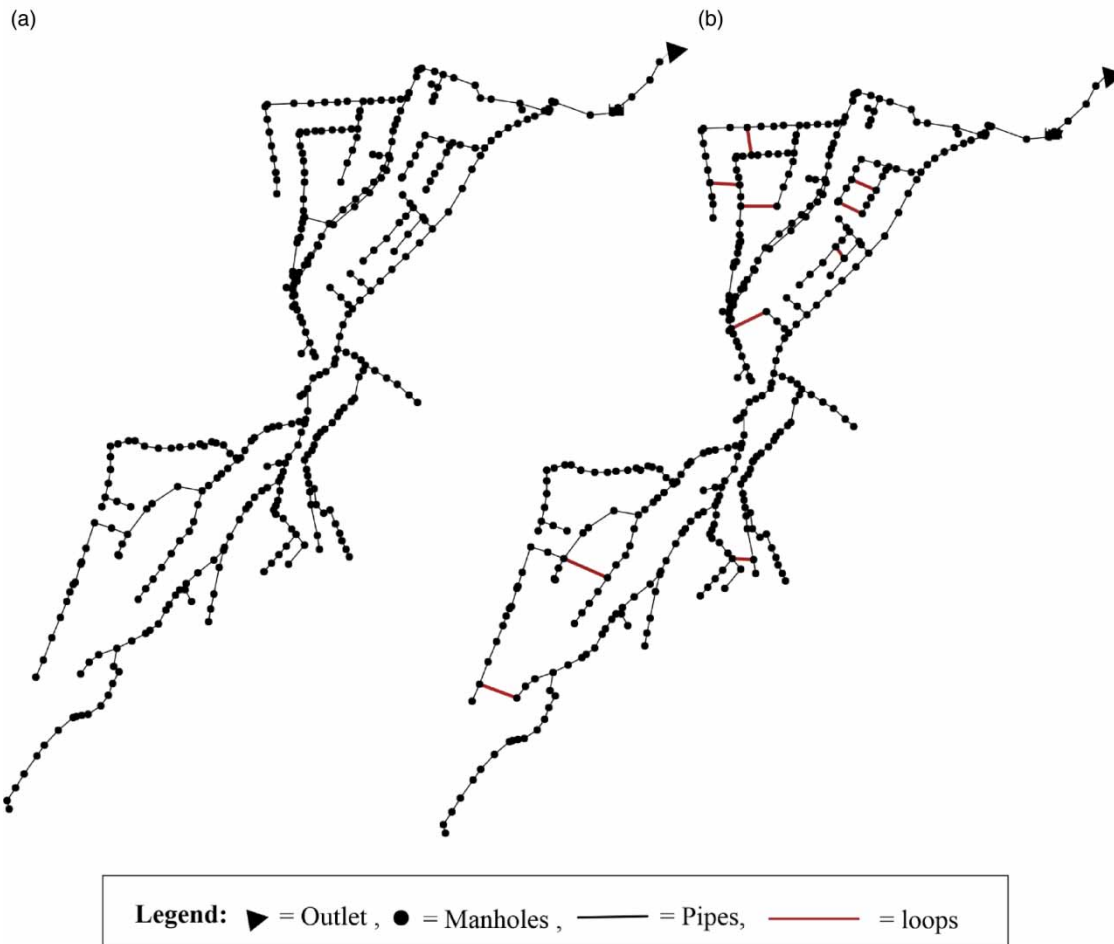


Figure 4 | (a) Original fully branched real network, (b) Looped real network.

to 1400 mm. The municipality has a population of 2931 inhabitants, and the network drains an area of 699 hectares. Similar to the benchmark network, in total 10 loops have been added manually to study the impact of loops on the proposed method.

Hardware and software

For hydrodynamic modelling, the Environmental Protection Agency (EPA's) Stormwater Management Model (SWMM) version 5.1 is used (Rossman 2010). For the application of graph-based method, Python's module Networkx version 2.6.2 developed specifically for network analysis is used (Hagberg *et al.* 2008). In terms of hardware, a laptop having an Intel[®] Core™ i7-10610 U CPU @ 2.3 GHz processor and 8 GB RAM is used. The system has a 64-bit Windows 10 operating system.

RESULTS AND DISCUSSION

In total five networks (three benchmark networks and two real networks) are analyzed by comparing GBM and HMM in terms of accuracy and computational time. A two-year return period rainfall was used for the three-benchmark network while a one-year return period block rain event was used for the two real networks. For evaluations, 25% most critical pipes (15 pipes) for small benchmark network and 5% most critical pipes (20 pipes) for the large real network are compared from both methods to analyze how well the graph method identifies the most critical parts of a stormwater network.

Branched networks

Figure 5 shows the difference between critical pipes identified by GBM and by HMM for a fully branched benchmark and real network. Figure 5(a) and 5(b) shows the 25% most critical pipes (15 pipes) highlighted in different colors according to the

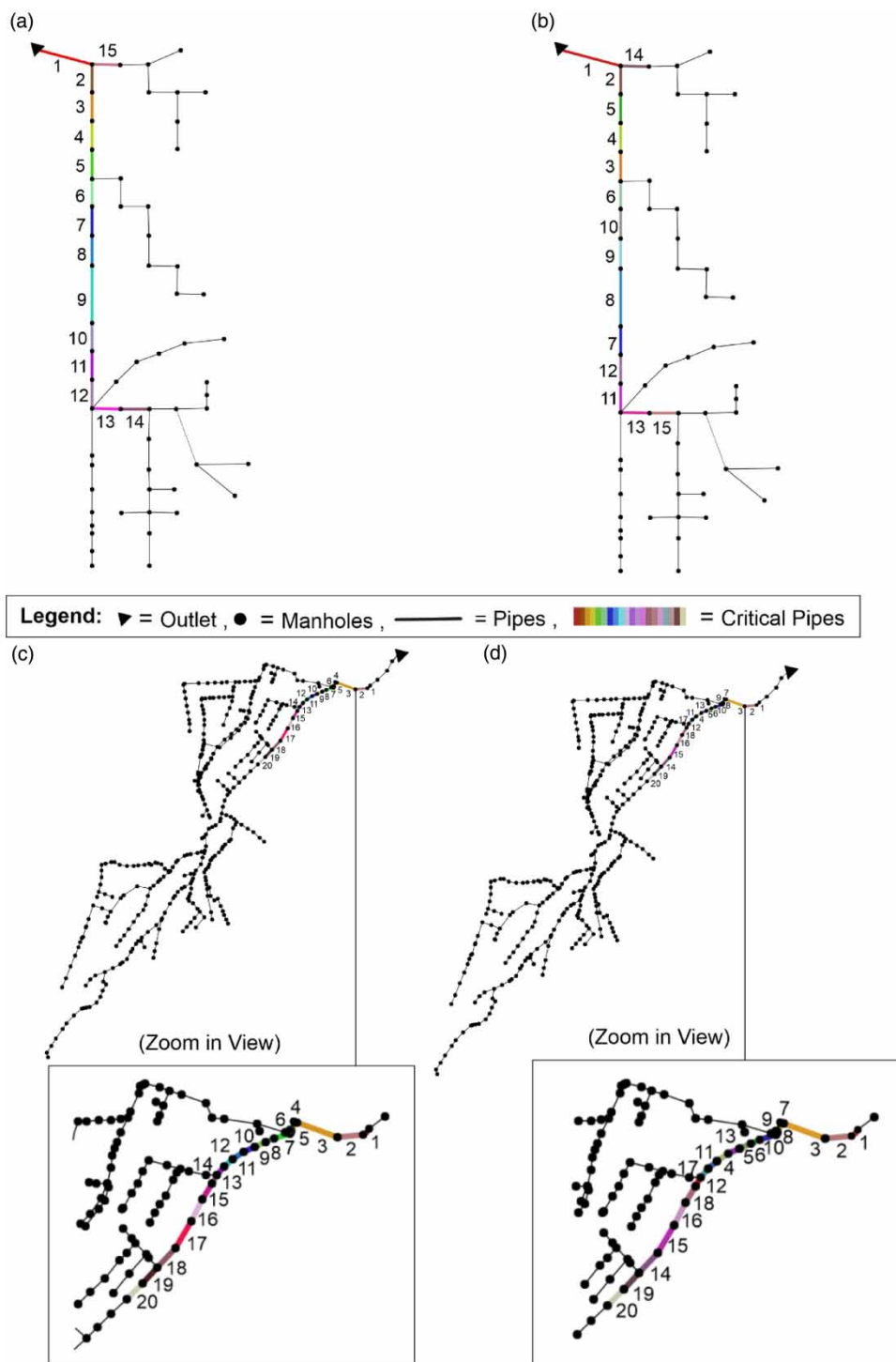


Figure 5 | Critical pipes shown in colors according to the order of criticality: (a) from graph method, benchmark network, (b) from HMM benchmark network, (c) from graph method, real network, (d) from HMM, real network.

order of criticality obtained from GBM and from the HMM respectively, for the benchmark network. In Figure 5(c) and 5(d), 5% most critical pipes (20 pipes) obtained from the GBM and HMM respectively, are highlighted in different colors according to the order of criticality of the pipes, for the real network. In both benchmark and real networks, all pipes identified critical by the HMM are also identified as critical by the proposed GBM. In addition, 33% of these critical pipes have the same order

of criticality in the case of benchmark network while 30% of the critical pipes have the same order of criticality for the real network.

It can be observed from these results that the proposed methodology has a high accuracy for branched networks both in the case of benchmark network and real network. The marginal differences in the results however, can be attributed to the fact that GBM does not include a detailed subcatchment hydrology like HMM does. Length, width and roughness of the subcatchments are incorporated in the method using runoff area of subcatchments (area * percentage imperviousness) in EBC_e^R concept. Also, the rainfall is added to the GBM model as a single value for the whole network and does not cater for the temporal variation of the rainfall while it is added as a 15 minutes block event in HMM.

Looped networks

Critical pipes identified by the two methods in the case of looped networks are given in Figure 6, colored according to their order of criticality, where (a) and (b) show the results for benchmark network with three loops for GBM and HMM respectively, (c) and (d) show results for benchmark network with six loops and (e) and (f) show the results for a real looped network for GBM and HMM respectively.

For a benchmark network with three loops and six loops, GBM identifies 12 out of 15 most critical pipes the same as HMM. This shows that the accuracy of the GBM decreases by the introduction of loops in the network. For a looped real network, GBM correctly identifies 19 out of 20 most critical pipes but the order of criticality is the same for only two of these 19 correctly identified pipes, again showing a decrease in accuracy as compared to branched real network results.

Difference between GBM and HMM flooding values

The above sections show the comparison of a few most important critical pipes using GBM and HMM visually through Figures 5 and 6. However, to understand the accuracy of GBM holistically, it is important to make a comparison of flooding volumes for all the pipes as well. This is done using NRMSE as described in the methodology section. NRMSE is used to compare the differences between flooding volume values from GBM and HMM for all five networks. Lower values of NRMSE indicate a small difference in the values from two methods. The values for NRMSE for all five networks are given in Table 4.

It can be seen from the table that for all networks the GBM results have differences as compared to HMM results. The major reason for that is HMM has a numerical solver where full Saint Venant flow equations are solved. The dynamic flow routing that is used in HMM can account for complex hydraulic behaviors like backwater effect, entrance/exit losses and flow reversal etc. On the other hand, GBM is a simple method that operates mostly based on the topology of the network while incorporating some hydraulic and functional properties indirectly. Hence, it is understandable that NRMSE values are not zero for any of the network. Another reason is that when a pipe is closed in HMM, there still remains water that resides in the system depending on the diameter and slope of the pipe. This water is not accounted for in GBM and hence GBM over-predicts flooding volumes as compared to HMM.

It can also be seen from NRMSE values that GBM flooding volume values are closest to HMM flooding volume values in the case of a branched real network. For the real network in general, GBM performs better than for the benchmark network. One of the main reasons for that is the benchmark network is a flat network with large, high capacity pipes and hence for a particular pipe that blocks, more water can remain in the system as compared to a real network which has smaller pipes and higher slopes.

Impact of loop degree

To better understand the impact of loop degree on the overall accuracy, a scatter plot shows flood volume from GBM and from HMM for both benchmark network and real network. Data fitting and correlation techniques are used to describe the impact of loop degree.

Figure 7 shows the plots comparing flood volumes from two methods for all five networks. The blue trendline in each graph shows the result of performing linear regression on the data. Coefficient of Determination (R^2) values are calculated from this linear regression and are also shown on the graphs for all five networks. It is evident from these results that the accuracy of GBM decreases with increasing loop degree. For the fully branched benchmark network, shown in Figure 7(a), the value of coefficient of determination is 0.98 which shows that the data has more than 98% correlation. This value decreases to 0.95 in the case of a network with 5% loop degree (three loops), shown in Figure 7(b) and to 0.92 in the case of a network with 10% loop degree (six loops), shown in Figure 7(c). This shows that increasing loop degree creates more complexity in the network and hence the accuracy of GBM is not as good as in the case of the fully branched network.

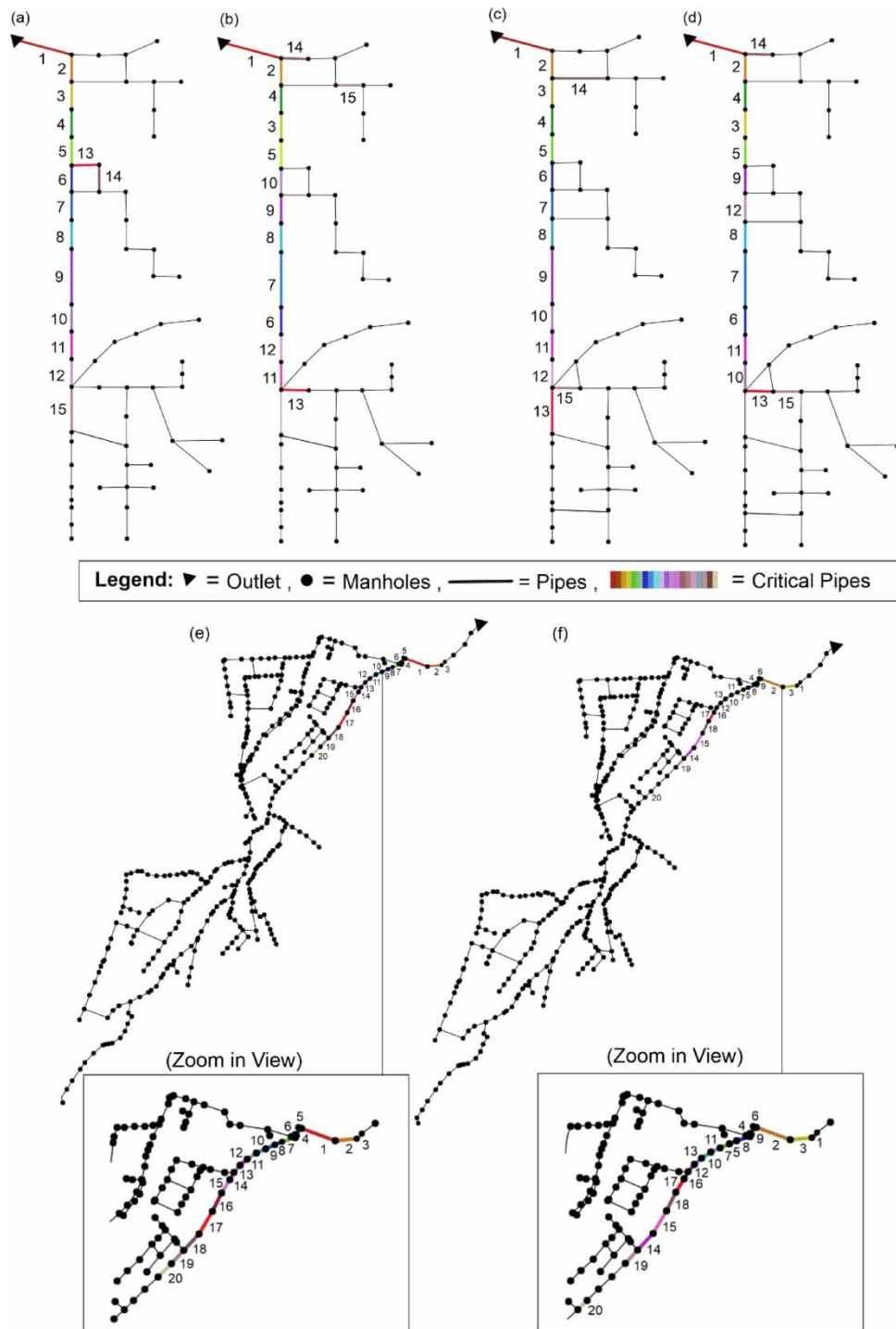


Figure 6 | Critical pipes shown in colors according to the order of criticality for benchmark network with three loops using: (a) GBM, (b) HMM, benchmark network with six loops using, (c) GBM, (d) HMM and looped real network using (e) GBM, (f) HMM.

This pattern is then also confirmed by repeating the same procedure for a real network. Again, the R-squared value reduces from 0.96 in the case of a branched network, shown in Figure 7(d), to 0.90 in the case of a looped network, shown in Figure 7(e), showing the loss in accuracy of proposed GBM. Here the decrease in accuracy is even more significant. For 3% loop degree added to the system, the correlation between the data reduces more significantly than the benchmark

Table 4 | Normalized root mean square error (NRMSE) values for all five networks

Network	NRMSE
Branched Benchmark Network	0.0834
Three Loops Benchmark Network	0.0987
Six Loops Benchmark network	0.1078
Branched Real Network	0.0361
Looped Real Network	0.0609

network. The reason is that the real network is a large and already complex network. Adding loops to this network increases its complexity even further, causing more significant loss in accuracy for GBM.

To further confirm these results, Pearson correlation coefficient (r) values calculated for all five networks are shown in Table 5. It can be seen that the ' r ' value follows the exact same pattern as R^2 values discussed above. The value of ' r ' for branched benchmark network is 0.99 which reduces to 0.97 in the case of a network with three loops and further decreases to 0.96 for a six loops benchmark network. For a real network, similar to R^2 values, the ' r ' value also decreases from 0.98 for a branched real network to 0.95 for a looped real network. Finally, NRMSE values increase with increasing loop degree which also confirm that the accuracy of GBM decreases with increasing loop degree.

The main reason behind the loss of accuracy for GBM when loops are added is the way how rerouting of water is being done in the graph method. The impact of rerouting of water in the proposed GBM is only considered for the adjacent pipes using EBC_c concept, while in reality this impact goes further downstream as well. Because of this simplification, the results for GBM become worse when the loop degree is increased. However, it can also be seen that even in looped networks the results of the proposed graph methodology are still sufficiently good (R-squared values greater than 0.9).

Impact of different return period rainfall

Another consideration for this study is how storm events with different return periods impact the performance of GBM. Fifteen minutes block rain is used with various return periods (i.e., 1, 2, 5, 10, 25, 50, and 100 years). R-squared value is determined between flooding from both methods for each return period and for both branched and looped real networks. The plot between R-squared values and return period is given in Figure 8. It can be seen that the R-squared values (accuracy of GBM as compared to HMM) decrease with the increasing return periods both for branched and looped networks. The reason is that the proposed methodology does not work very well when the system is pressured with higher return period rainfall. One of the reasons for that is the capacity considerations is not part of the GBM in this study which means if there is already flooding because of lack of capacity (which is the case for higher return period rain), GBM will not predict the flooding as well as HMM. The branched network has a more significant drop in R-squared values and hence in the accuracy of GBM as compared to a looped network. This shows that for a branched network hydraulic modelling gives much better results in the estimation of flood flows when the system is modelled for higher rainfall than graph methodology (coefficient of determination as low as 0.56 for 100-year return period rain). However, for the looped network, performance of graph method is more comparable to that of HMM, even for higher rain, as the coefficient of determination values do not go under 0.7.

Computational time and data requirements

Table 6 shows the comparison of computational time taken by GBM and HMM. In the case of a benchmark network, HMM takes 5 minutes and 20 seconds to run. As it is an iterative method, the model has to run once for each pipe blockage scenario. In comparison, GBM only takes 6 seconds to run having a computational gain factor of 53 (320/6) as compared to HMM. The benefit of computational time increases with the size of the network, because running HMM takes significantly more time for larger and more complex networks. For example, HMM takes 45 minutes to run for real network, while GBM takes only 10 seconds with very little attention to code efficiency. The computational gain factor in the case of real case study is hence 270 (45*60/10). Subsequently, the computational gain factor between the two methods increases significantly with increasing network size. Thus, the graph method is much more efficient in the case of large USNs and when a lot of simulations have to be run.

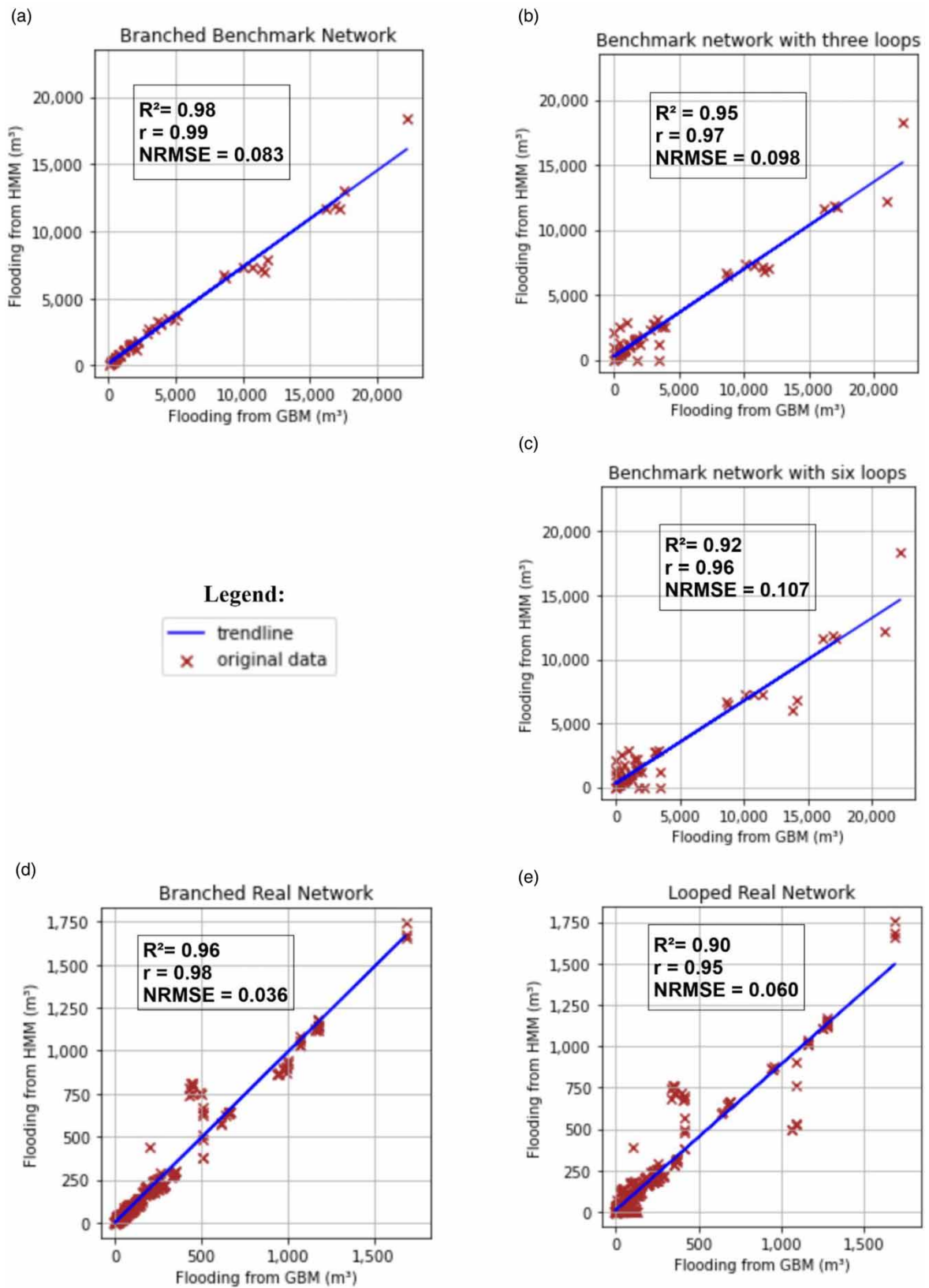
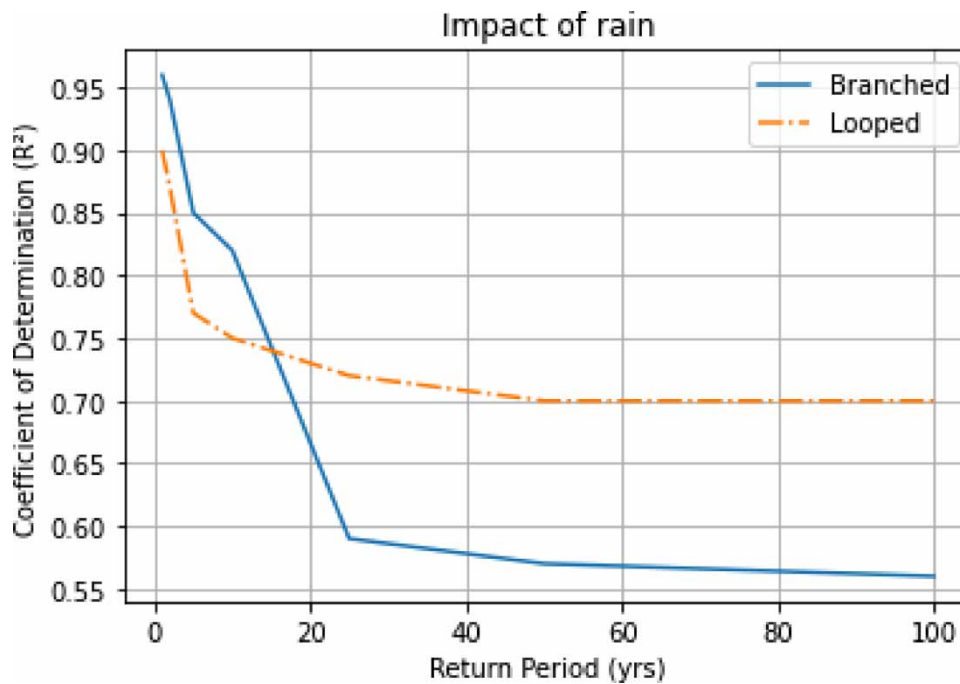


Figure 7 | Comparison of flooding from GBM and HMM for: (a) Benchmark branched network, (b) Benchmark three loops network, (c) Benchmark six loops network, (d) Real branched network, (e) Real looped network.

Table 5 | Values of the three statistical coefficients for all five networks

Network	NRMSE	r	R ²
Branched Benchmark Network	0.0834	0.99	0.98
Three Loops Benchmark Network	0.0987	0.97	0.95
Six Loops Benchmark Network	0.1078	0.96	0.92
Branched Real Network	0.0361	0.98	0.96
Looped Real Network	0.0609	0.95	0.90

**Figure 8** | Graph showing impact of different return period rainfall for real branched and looped network.**Table 6** | Comparison of computational time taken for GBM and HMM

Network	GBM	HMM	Computational gain factor
Benchmark	6 seconds	320 seconds	$(320/6) = 53$
Real	10 seconds	2700 seconds (45 mins)	$(2700/10) = 270$

Hybrid simulations involving both graph methodology and hydrodynamic simulations were also considered to figure out the computational gain and accuracy in that case. The 20 most critical pipes were found using GBM and then HMM was used to evaluate the criticality of these 20 pipes. The hybrid simulations were performed for branched real case study. The accuracy of hybrid simulations in this case is 100%. It identifies all 20 pipes and in the same order of criticality, but the computational time is significantly less as compared to HMM because in this case only 20 iterations of hydrodynamic simulations are required. The hybrid method takes around 3 minutes to run (10 seconds for GBM and 8*20 for HMM simulations) as compared to 45 minutes of HMM having a computational gain factor of 15 over HMM.

GBM can be setup with just nodes, links and sub catchments data. On the other hand, setting up a full scale urban hydrodynamic model requires more data including, soil information, land use, etc. Hence, GBM presented in this study is less data-

intensive as compared to conventional HMM. Additionally, it is also easier and less time-consuming to set up the graph method as compared to setting up a full-scale hydrodynamic model. Once the code is ready for running the graph methodology, it can be used for different case studies by making minor, quick changes, while the hydrodynamic model has to be set up from scratch every time.

Advantages, limitations and future work

GBM has a number of advantages over other commonly used models, e.g. conceptual hydrological model including GBM directly converts the network to a graph and structural and layout details are very well preserved. GBM can be adapted to a higher level of combinatorial problems very easily and can be used to test other graph metrics. It is also a non-iterative method, so it takes less computational effort, the methodology is easy to implement and can be extended to multiple pipe failure. The methodology can be used for specific practical use cases, for example when a lot of simulations or scenarios are required, e.g. deep uncertainty analysis, future developments, multiple pipe failure combinations etc., or when the complete data is not available to setup the full hydrodynamic model.

The GBM described in this study has some limitations as well. For instance, our proposed framework is not able to model complex hydraulic behaviors like the backwater effect resulting from the blocked pipes. In addition, rerouting of water in case of presence of loops is simplified by the GBM while in reality it is much more complex. This implies that the rerouting can affect the pipes further downstream as well, which is not yet modeled using GBM. This also explains the decrease in accuracy of the method as more and more loops are added.

Future work in this regard will focus on extending the proposed GBM to more diverse real-life case studies. Capacity considerations will also be added to the methodology. Impact of hydraulic structures on GBM and how they can be incorporated without compromising accuracy will also be part of the future work. One of the next steps in this research is to further explore the potential of a hybrid graph and hydrodynamic modelling approach. Additionally, the research will also be extended to multiple pipe failure scenarios and potentially to cascading failures using GBM.

CONCLUSIONS

In this study, a new graph-based methodology (GBM) is proposed based on so-called runoff edge betweenness centrality (EBC_e^R) as a measure to identify most critical pipes of urban stormwater networks (USNs). The method uses network analysis techniques adapted to USN to mimic the hydraulic and functional properties. The method does not include the capacity problems of the initial system; hence it is important that the base flooding in the initial system is zero. Key findings of the study are mentioned below:

- Results indicate that the graph method is highly accurate in case of branched networks, R^2 value of 0.98 and ' r ' value of 0.99 for benchmark network. The value decreases to $R^2 = 0.96$ and $r = 0.98$ in the case of branched real network which is larger and more complex showing that the increasing complexity and size of USN slightly reduces the accuracy of the method.
- Normalized root mean square error values for all five networks show that the real network performs better than the benchmark network, specifically the branched real network has the least differences between flooding volumes from two methods.
- Impact of loop degree on the methodology is also studied in this research. The results show that the accuracy of methodology decreases by introducing loops. Furthermore, GBM becomes less accurate with increasing loop degree as is clear from the case of benchmark network.
- Real network is used to study the impact of higher return period rain on GBM. The results indicate that the accuracy of the methodology decreases with increasing return periods showing that the method does not work very well when the system is already flooding because of lack of capacity.
- Although the accuracy of graph methodology is not as good as HMM, the biggest advantage of using GBM lies in the difference in the computational time required to run both methodologies. GBM has a computational gain factor of 53 for benchmark network which increases to 270 for the real network. This shows that not only the proposed GBM is efficient in terms of computational time but also the efficiency increases as the size of the network increases.
- Also, GBM is less data intensive and is easier to setup as compared to a full-scale hydrodynamic model. Especially for larger networks and more scenarios (e.g., cascading failures, failure combinations), GBM can provide results in more reasonable time.

- Additionally, a hybrid method based on both graph methodology and hydrodynamic simulations can be used to find out critical pipes of a USN with higher accuracy as compared to GBM and in significantly less time as compared to HMM.
- The proposed GBM in this paper can be used by small utilities where a quick initial and preliminary analysis is required or where the data available is not enough to setup a hydrodynamic model. Moreover, in the case of large cities with large-scale USNs where running multiple simulations of conventional hydrodynamic model becomes too time-consuming, the proposed methodology can be promising.

ACKNOWLEDGEMENTS

This study is funded by Austrian Science Fund (FWF) P 31104-N29

DATA AVAILABILITY STATEMENT

All relevant data are included in the paper or its Supplementary Information.

CONFLICT OF INTEREST

The authors declare there is no conflict.

REFERENCES

- Arthur, S. & Crow, H. 2007 Prioritising sewerage maintenance using serviceability criteria. *Proceedings of the Institution of Civil Engineers – Water Management* **160** (3), 189–194.
- Butler, D., Ward, S., Sweetapple, C., Astaraie-Imani, M., Diao, K., Farmani, R. & Fu, G. 2017 Reliable, resilient and sustainable water management: the Safe & SuRe approach. *Global Challenges* **1** (1), 63–77.
- Dijkstra, E. W. 1959 A note on two problems in connexion with graphs. *Numerische Mathematik* **1** (1), 269–271.
- Dong, X., Guo, H. & Zeng, S. 2017 Enhancing future resilience in urban drainage system: green versus grey infrastructure. *Water Research* **124**, 280–289.
- Fu, G., Butler, D., Khu, S.-T. & Sun, S. A. 2011 Imprecise probabilistic evaluation of sewer flooding in urban drainage systems using random set theory. *Water Resources Research* **47** (2), 534.
- Gioia, G. & Bombardelli, F. A. 2001 Scaling and similarity in rough channel flows. *Physical Review Letters* **88** (1), 014501.
- Hagberg, A. A., Schult, D. A. & Stewart, P. J. 2008 Exploring network structure, dynamics and function using NetworkX. *SciPy* **7**, 11–15.
- Hajibabaei, M., Yousefi, A., Hesarkazzazi, S., Roy, A., Hummel, M. A., Jenewein, O., Shahandashti, M. & Sitzenfrei, R. 2022 Identification of critical pipes of water distribution networks using a hydraulically informed graph-based approach. *World Environmental and Water Resources Congress* **2022**, 1041–1053.
- Hesarkazzazi, S., Hajibabaei, M., Diao, K. & Sitzenfrei, R. 2021 Implication of different pipe-sizing strategies for the resilience of stormwater networks. *World Environmental and Water Resources Congress* **2021**, 244–252.
- Hesarkazzazi, S., Bakhshipour, A. E., Hajibabaei, M., Dittmer, U., Haghghi, A. & Sitzenfrei, R. 2022a Battle of centralized and decentralized urban stormwater networks: from redundancy perspective. *Water Research* **222**, 118910.
- Hesarkazzazi, S., Hajibabaei, M., Bakhshipour, A. E., Dittmer, U., Haghghi, A. & Sitzenfrei, R. 2022b Generation of optimal (de)centralized layouts for urban drainage systems: a graph-theory-based combinatorial multi-objective optimization framework. *Sustainable Cities and Society* **81**, 103827.
- Le Gauffre, P., Joannis, C., Vasconcelos, E., Breyse, D., Gibello, C. & Desmulliez, J.-J. 2007 Performance indicators and multicriteria decision support for sewer asset management. *Journal of Infrastructure Systems* **13** (2), 105–114.
- Mair, M., Sitzenfrei, R., Kleidorfer, M., Möderl, M. & Rauch, W. 2012 GIS-based applications of sensitivity analysis for sewer models. *Water Science and Technology* **65** (7), 1215–1222.
- Meijer, D., Van Bijnen, M., Langeveld, J., Korving, H., Post, J. & Clemens, F. 2018 Identifying critical elements in sewer networks using graph-theory. *Water* **10** (2), 136.
- Möderl, M. & Rauch, W. 2011 Spatial risk assessment for critical network infrastructure using sensitivity analysis. *Frontiers of Earth Science* **5** (4), 414–420.
- Möderl, M., Kleidorfer, M., Sitzenfrei, R. & Rauch, W. 2009 Identifying weak points of urban drainage systems by means of VulNetUD. *Water Science and Technology* **60** (10), 2507–2513.
- Mugume, S. N. & Butler, D. 2017 Evaluation of functional resilience in urban drainage and flood management systems using a global analysis approach. *Urban Water Journal* **14** (7), 727–736.
- Mugume, S. N., Diao, K., Astaraie-Imani, M., Fu, G., Farmani, R. & Butler, D. 2015 Enhancing resilience in urban water systems for future cities. *Water Supply* **15** (6), 1343–1352.
- Pagano, A., Sweetapple, C., Farmani, R., Giordano, R. & Butler, D. 2019 Water distribution networks resilience analysis: a comparison between graph theory-based approaches and global resilience analysis. *Water Resources Management* **33** (8), 2925–2940.

- Pearson, K. 1895 Notes on regression and inheritance in the case of two parents. *Proceedings of the Royal Society of London* **58**, 240–242.
- Reyes-Silva, J. D., Zischg, J., Klinkhamer, C., Rao, P. S. C., Sitzenfrei, R. & Krebs, P. 2020 Centrality and shortest path length measures for the functional analysis of urban drainage networks. *Applied Network Science* **5** (1), 1.
- Rossman, L. A. 2010 *Stormwater Management Model, User Manual, Version 5.0*. U.S Environmental Protection Agency, Cincinnati, OH, USA.
- Sitzenfrei, R., Mair, M., Möderl, M. & Rauch, W. 2011 Cascade vulnerability for risk analysis of water infrastructure. *Water Science and Technology* **64** (9), 1885–1891.
- Sitzenfrei, R., Urich, C., Möderl, M. & Rauch, W. 2013 Assessing the efficiency of different CSO positions based on network graph characteristics. *Water Science and Technology* **67** (7), 1574–1580.
- Sitzenfrei, R., Wang, Q., Kapelan, Z. & Savić, D. 2020 Using complex network analysis for optimization of water distribution networks. *Water Resources Research* **56** (8), e2020WR027929.
- Turan, M. E., Bacak-Turan, G., Cetin, T. & Aslan, E. 2019 Feasible sanitary sewer network generation using graph theory. *Advances in Civil Engineering* **2019**, 8527180.
- Zhang, C., Wang, Y., Li, Y. & Ding, W. 2017 Vulnerability analysis of urban drainage systems: tree vs. loop networks. *Sustainability* **9** (3), 397.

First received 22 August 2022; accepted in revised form 5 December 2022. Available online 17 December 2022